BNL-223886-2023-JAAM

# Investigation of signal characteristics and charge sharing in AC-LGADs with laser and test beam measurements

J. Ott, W. Chen

To be published in "NUCLEAR INSTRUMENTS & METHODS IN PHYSICS RESEARCH SECTION A-ACCELERATORS SPECTROMETERS DETECTORS AND ASSOCIATED EQUIPMENT"

January 2023

Instrumentation Division

**Brookhaven National Laboratory**

**U.S. Department of Energy**

USDOE Office of Science (SC), High Energy Physics (HEP) (SC-25)

# DISCLAIMER

# Investigation of signal characteristics and charge sharing in AC-LGADs with laser and test beam measurements

J. Ott[a,], S. Letts[a], A. Molnar[a], E. Ryan[a], M. Wong[a], S. Mazza[a], M. Nizam[a], H. F.-W. Sadrozinski[a], B. Schumm[a], A. Seiden[a], T. Shin[a], Ryan Heller[b], Christopher Madrid[b], Artur Apresyan[b], William K. Brooks[g,h,i], Wei Chen[c], Gabriele D'Amen[c], Gabriele Giacomini[c], Ikumi Goya[e], Kazuhiko Hara[e], Sayuka Kita[e], Sergey Los[b], Koji Nakamura[d], Cristián Peña[b], Claudio San Martín[g,1], Tatsuki Ueda[e], Alessandro Tricoli[c], Si Xie[b,f]

[a]*Santa Cruz Institute for Particle Physics, University of California at Santa Cruz, 1156 High Street, Santa Cruz CA 95064, USA*
[b]*Fermi National Accelerator Laboratory, PO Box 500, Batavia IL 60510-5011, USA*
[c]*Brookhaven National Laboratory, Upton, 11973, NY, USA*
[d]*High Energy Research Organization, Oho 1-1, Tsukuba, Ibaraki, 305-0801, Japan*
[e]*University of Tsukuba, 1-1-1 Tennodai, Tsukuba, Ibaraki, 305-8571, Japan*
[f]*California Institute of Technology, Pasadena, CA, USA*
[g]*Departamento de Física y Astronomía, Universidad Técnica Federico Santa María,Valparaiso, Chile*
[h]*Centro Científico Tecnológico de Valparaíso-CCTVal, Universidad Técnica Federico Santa María, Casilla 110-V, Valparaíso, Chile*
[i]*Millennium Institute for Subatomic Physics at the High-Energy Frontier (SAPHIR) of ANID, Fernández Concha 700, Santiago, Chile*

**Abstract**

AC-LGADs, also referred to as resistive silicon detectors, are a recent development of low-gain avalanche detectors (LGADs), based on a sensor design where the multiplication layer and $n^+$ contact are continuous, and only the metal layer is patterned. In AC-LGADs, the signal is capacitively coupled from the continuous, resistive $n^+$ layer over a dielectric to the metal electrodes. Therefore, the spatial resolution is not only influenced by the electrode pitch, but also the relative size of the metal electrodes. Signal propagation between the metallized areas and charge sharing between electrodes plays a larger role in these detectors than in conventional silicon sensors read out in DC mode. AC-LGADs from two manufacturers were studied in beam tests and with infrared laser scans. The impact of $n^+$ layer resistivity and metal electrode pitch on the charge sharing and achievable position resolution is shown. For strips with 100 µm pitch, a resolution of $< 6$ µm can be reached. The charge sharing between neighboring strips is investigated in more detail, indicating the induction of signal charge and subsequent re-sharing over the $n^+$ layer. Furthermore,

*Email address:* `jeott@ucsc.edu` (J. Ott)

an approach to identify signal sharing over large distances is presented.

*Keywords:* ultrafast timing, AC-LGAD, charge sharing, beam test

---

## 1. Introduction

Low-gain avalanche diodes (LGADs) are silicon sensors with low to moderate gain on the order of 5-50. LGADs can reach a timing resolution of 18-20 ps and are typically implemented on thin (30-80 µm) active p-type substrates with an $n^+$ implant on the readout side, with the gain provided by an additional boron-doped $p^+$ multiplication layer below the top electrode.[1, 2, 3] A recent development in ultrafast silicon sensor technology are AC-coupled LGADs, also referred to as Resistive Silicon Detectors (RSD)[4], in which the signal is read out from metal pads on top of a continuous layer of oxide, and the underlying charge-collecting n+ implant is contacted only by a separate biasing contact.[1, 5] As the implant and gain layers can be continuous, the challenging termination of the gain layer at the edges of each segment is not required anymore and the inactive regions within the sensor area are eliminated. Furthermore, the spatial resolution of hits in sensors with a continuous implant layer can be improved by analyzing and interpolating the signal sharing between the metal pads.

AC-LGAD sensors produced by Hamamatsu P.K. (HPK) and at Brookhaven National Laboratory (BNL) were the subject of a test beam campaign at Fermilab[6]. This article focuses on examining various aspects of charge sharing in some of these sensors. First, the impact of $n^+$ resistivity and strip pitch on the charge sharing, and thus position resolution, is shown. Afterwards, the shape of the maximum signal amplitude profile over the sensor is studied more closely, and a comparison to data obtained in the laboratory with a laser is displayed. Finally, the distinction of charge shared of a real signal from noise by the application of timing cuts is introduced.

## 2. Experimental

### *2.1. Sensors*

Two different types of AC-LGAD sensors, a pad sensor produced by HPK and a strip sensor fabricated by BNL, were studied.

The BNL2021 AC-LGAD strip sensor [5] has an active thickness of 50 $\mu$m, active area of 3 $\times$ 3 mm$^2$ and ca. 2.5 mm strip length. The strip metal width is kept constant, while the pitch is varied over three groups of strips. A photograph of the sensor, with frames indicating the different pitches, is shown in Fig 1. The strip parameters are listed in Table 1. The $n^+$ doping concentration is approximately 100 times less than in a standard DC-LGAD. The sensor was biased at -285 V.

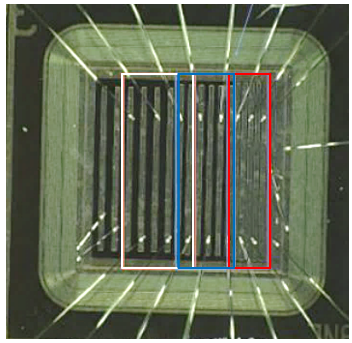

Figure 1: BNL2021 AC-LGAD strip sensor. Channels read out for each pitch are marked with red (Narrow), blue (Medium) and white (Wide).

Table 1: BNL2021 strip parameters.

| Label | **Narrow** | **Medium** | **Wide** |
|---|---|---|---|
| Pitch [$\mu$m] | 100 | 150 | 200 |
| Metal width [$\mu$m] | 80 | 80 | 80 |
| Distance between metal edges [$\mu$m] | 20 | 70 | 120 |

The investigated HPK AC-LGADs also has an active thickness of 50 µm and total active area of 3 × 3 mm$^2$, but features a 2 × 2 pad geometry instead of strips. The pad size is constant with 500 × 500 µm$^2$, with different interpad gap widths between each of the pads. The channels studied here had a gap of 50 µm. The n$^+$ layer resistivity and gain layer doping in the HPK production is denoted with a letter-number combination; here, sensors B2 and C2 were studied, corresponding to an n+ doping concentration of 3.3 and 10 times less than a typical DC-LGAD, respectively.[7] The sensors were biased at -230 and -180 V.

### *2.2. Characterization*

Sensors were mounted on 16-channel fast analog amplifier boards with 1 GHz bandwidth, designed at Fermilab.

At the Fermilab Test Beam Facility [8], the sensors were tested with a 120 GeV proton beam. The position of the proton tracks was determined with the FTBF silicon beam telescope, consisting of 3 upstream and 4 downstream layers of pixel detectors, as well as 4 downstream layers of strips, providing a combined resolution of 5-10 um. A Photek micro-channel plate detector (MCP-PMT) with a time resolution of ca. 10 ps was used as reference for the proton arrival time. The signals were read out with a Lecroy Waverunner 2 GHz, 10 GS/s oscilloscope.[6]

In the laser Transient Current Technique (TCT) measurements, the sensors were excited with a 1064 nm infrared (IR) laser. The IR laser has a penetration length in silicon of several mm causing a linearly distributed ionization throughout the bulk. The laser beam was focused by a lens system to a spot size of ca. 20 µm at the focal point, and the laser power was adjusted to mimic the response of the sensor to a minimum-ionizing particle. The analog board was mounted on an X-Y moving stage to enable 2D mapping scans. The sensors were read out by a Lecroy Waverunner oscilloscope (2 GHz, 20 GS/s). For each point in the scan, an average waveform (100 events) was registered for each readout channel to decrease the impact of variations in the laser power as well as noise.

## 3. Results and Discussion

### *3.1. Position resolution*

Due to the common resistive $n^+$ layer, signal sharing between neighboring channels in AC-LGADs can be used to reconstruct the position of a hit to a better precision than in a traditional binary readout, where the position resolution is given by pitch/$\sqrt{12}$. This method is based on the maximum pulse amplitude (pmax) observed in several channels, and its change with hit position.

The pmax fraction of a channel is calculated as:

$$Fraction_{ch} = \frac{pmax_{ch}}{\sum pmax} \tag{1}$$

Here, the position reconstruction is based on two adjacent channels. The pmax fraction as function of position is calculated directly from the experimental data, and is fitted with an error function to replicate the s-shaped curve of the data. Extracting d(Position) and d(Fraction) from this fit, and using the summed pmax and RMS noise of the respective channel in the signal-to-noise ratio, the position resolution is determined as:

$$\sigma_{pos} = \sqrt{2}\frac{d(Position)}{d(Fraction)}/\frac{S}{N} \tag{2}$$

In the following, the centered zero position refers to the middle of the gap between strips, and the data ends at the respective center of the two channels used in the pmax evaluation.

### *3.1.1. Impact of $n^+$ implant in HPK pad sensors*

In Figure 2 a direct comparison of the charge sharing (in terms of pmax fraction of two neighboring pads) and the resulting position resolution, determined with Eq.2, is shown for HPK B2 and C2 pad sensors. The slope of the pmax fraction is clearly steeper in the C2 sensor, which features the higher $n^+$ resistivity [7]. A similar result was indicated in [6], comparing MPV signal amplitudes. The reduced charge sharing in the C2 sensor translates into a better position resolution, with 7.5 µm in the center between pads, as opposed to the B2 sensor which reaches 16.5 µm at minimum. It is visible that the position resolution is not uniform over the examined position: the smaller the change in pmax fraction, which levels out to almost constant under the metal pad, the worse the position resolution reconstructed with this method becomes. This implies that very large metal pads do not provide an improved position resolution over most of the position range. No variation of the n+ layer resistivity was available for the BNL2021 strip production. Ongoing and near-future test beam campaigns including strip sensors from HPK may allow an evaluation of charge sharing depending on $n^+$ layer resistivity.

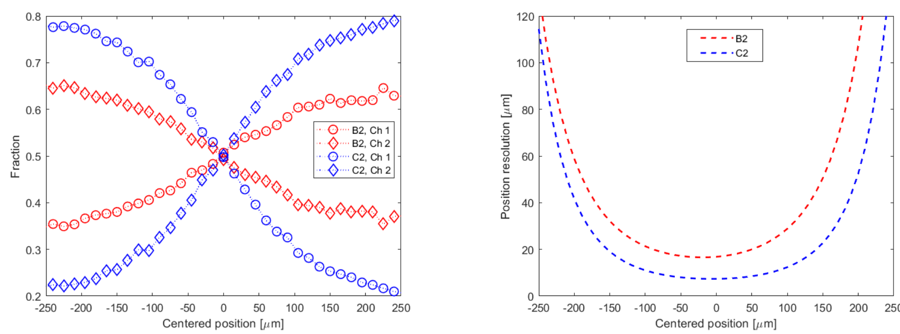


(a) (b)

Figure 2: a) pmax fraction and b) position resolution of HPK AC-LGAD pad sensors B2 and C2. Charge sharing is more defined and position resolution lower for the C2 sensor with higher $n^+$ layer resistivity.

### *3.1.2. Impact of the pitch on charge sharing in strip sensors*

Figure 3 presents pmax fractions and calculated position resolution as function of position for the BNL2021 strip sensor and its three different strip pitches.

The strip pitch is expected to, and appears to, have a large impact on charge sharing as seen in the pmax fraction curve. Indeed, between the two strips used for position reconstruction, the best resolution is determined as ca. 4 µm, 4.5 µm and 5.5 µm for Narrow, Medium and Wide pitch, respectively. At best, this corresponds to $< 1/20$ of the pitch. On the other hand, the position resolution of ca. 15 µm at the respective strip metal centers is in fact very similar for all three strip pitches.

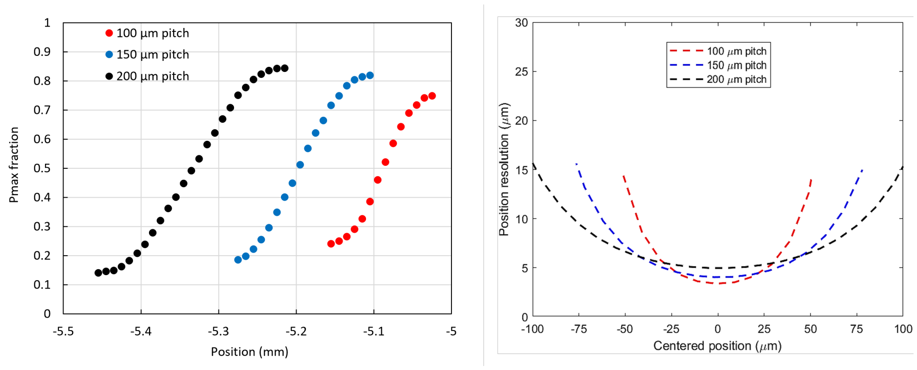


Figure 3: Pmax fraction (left) and position resolution (right) of BNL2021 AC-LGAD strip sensor with different pitches.

### 3.2. *Charge sharing in neighboring strips*

Figure 4 shows pmax averages as function of position on the sensor over a group of strips, here for the Medium pitch. It is noticeable that the profile is not a smooth curve, but exhibits a widening roughly at the center of the adjacent strips.

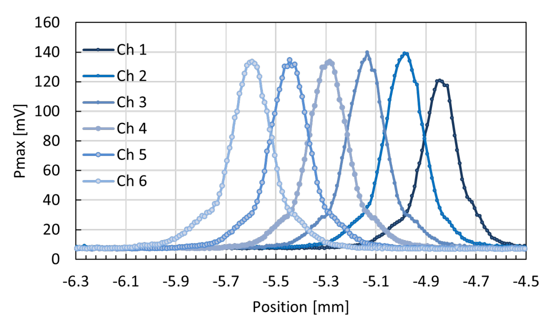


Figure 4: Pmax profiles for several channels of a Medium (150 µm) pitch on the BNL2021 AC-LGAD strip sensor.

Figures 5 and 6 show the fitting of the pmax profile as function of position, for the example case of Ch 4, for different pitches. Fitting the data (after subtraction of a constant floor of ca. 7 mV) with multiple Gaussians reveals that the measured pmax consists of several contributions. For the Narrow, 100 µm pitch, the overall pmax profile is explained by the contributions from both next neighbors and even second neighbors. Here, the actual sharing extends from the central strip almost to the far edge of the second neighbor. For Medium, 150 µm, no clear contribution from the second neighbors can be reliably identified using the available statistics, but the contributions from the immediate neighbors are larger than for the Wide, 200 µm pitch strips. The localization of the contributions - i.e., not exhibiting a smooth, single-Gaussian shape for pmax on the strip - indicates that the charge on the metal is not shared purely by conduction through the resistive $n^+$ layer from the channel under investigation, but that the charge generated by an impacting particle induces a signal on the neighboring strips already during the drift of the carriers in the bulk, which is then subsequently shared over the $n^+$. This needs to be verified by further investigation, including device simulations, to separate the impact of signal induction and the potential additional impact of the common $n^+$ layer especially on charge sharing between strips at longer distances.

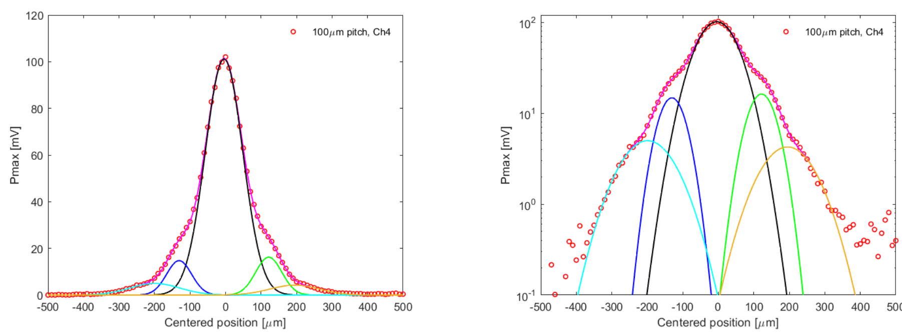


(a) (b)

Figure 5: BNL2021 AC-LGAD Narrow (100 µm) pitch strip pmax profile, fitted with multiple Gaussians: a) linear, b) logarithmic y-axis.

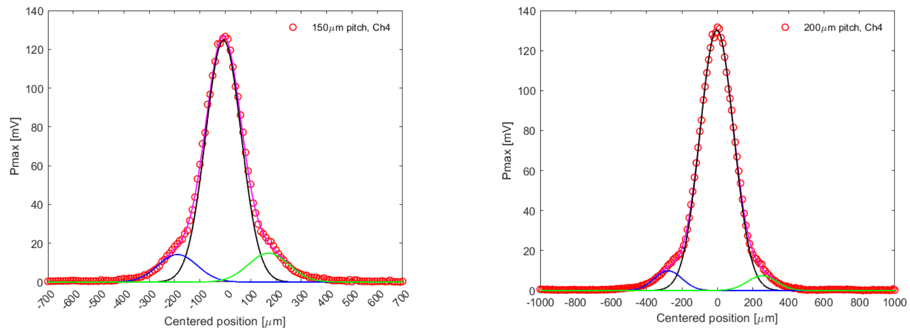


(a) (b)

Figure 6: BNL2021 AC-LGAD pmax profile and fits with multiple Gaussians: a) Medium, 150 µm pitch, b) Wide, 200 µm pitch strips.

### *3.3. Investigation of charge sharing with laser data*

It is shown in [9] that the position resolution can be determined by two-channel reconstruction also from laser data. However, these measurements were conducted on pad sensors with wider openings in the metal compared to the BNL2021 strip sensor. For an accurate reconstruction, the laser measurement data in the areas under the metal (where it the signal is zero or near-zero) needs to be manually excluded from the calculation.

When overlaying the laser and beam test data for the same sensor geometry (Fig. 7), normalizing the pmax profiles to the maxima for their respective pitch, the laser data shows similar trends as the test beam study. However, in the BNL2021 strip sensor, the gap between strips ranges from 20 $\mu$m (Narrow) to 120 $\mu$m (Wide) - considering also the width of the laser beam spot, at ca. 15-20 $\mu$m at the focal point, it would not be possible to discover the contributions to the pmax profile from the neighboring strips in this sensor geometry by laser data alone, especially for the Narrow pitch. Consequently, a thorough understanding of charge sharing in AC-LGAD still relies heavily on measurements in a test beam.

It should be noted that due to the waveform averaging, the noise in the laser data appears to be zero. In the beam test, signal sharing over very large distances may be hidden in the baseline offset, which was again subtracted for this comparison.

### *3.4. Separation of signals and noise by in-time/out-of-time classification*

In order to distinguish between charge originating from an actual signal, and the noise or time-independent pick-up in a channel, the timing of the automatically computed pmax was employed.

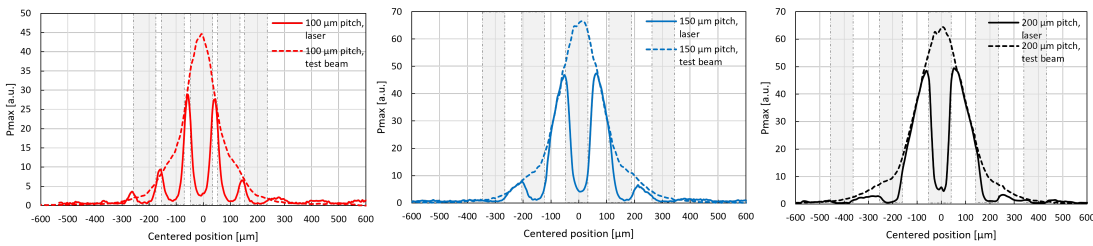


Figure 7: BNL strip pmax profiles, overlay of test beam (dashed line) and laser data (solid line): a) Narrow, 100 $\mu$m, b) Medium, 150 $\mu$m, c) Wide, 200 $\mu$m pitch. Strip metallization is indicated in grey.

For this purpose, only events with a large pulse height of 125-135 mV in a central channel (Ch 4 of each pitch) were considered. No cuts were applied on the other channels. The data classified as "in-time" was as pmax distribution in a 1 ns window around the main signal's typical time stamp relative to the timing reference. The "out-of-time" data was averaged over three 1 ns time bins before the signal time window, in order to exclude potentially higher noise of the channel immediately after the signal.

In-time and out-of-time pmax distributions were analysed with Gaussian and Landau fits, as well as through the median values of the distributions. The analysis method did not have a significant impact on the result. The Gaussian distribution was chosen as most suitable representation.

The respective in-time and out-of-time pmax values (i.e., resulting centroid channels of Gaussian distribution fit) for different pitches are shown in Fig. 8. This result demonstrates that even 2-3 channels and several hundreds of µm away from the hit and the channel with the largest part of the signal, a small signal component above the noise level, as determined by in-time/out-of time pmax values, is observed. For a narrower pitch, more charge is visible on the nearest neighbors. One one hand, this is clear evidence of the charge sharing in AC-LGADs and that even small signals can be identified far away from the particle track; on the other hand, charge sharing over very long distances may contribute to elevated background levels for other events, which is detrimental especially in environments with higher hit rates and luminosities.

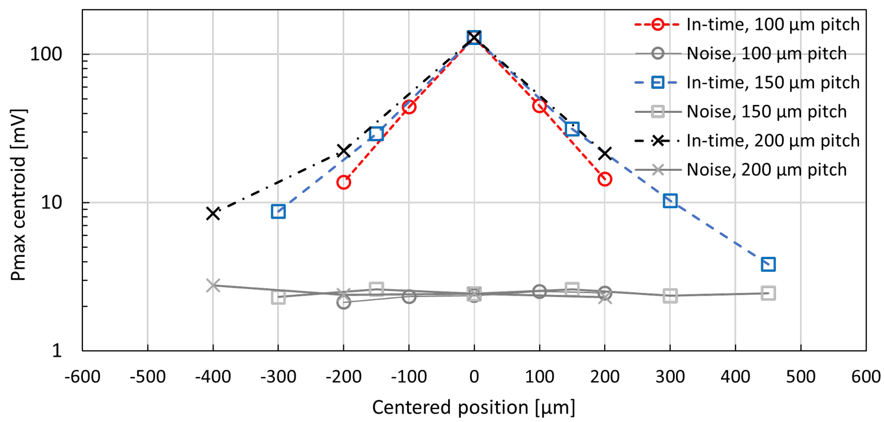


Figure 8: Pmax as function of position, for events with pmax of 125-135 mV on Ch 4. In-time values are indicated in color for different pitches, out-of-time (noise) levels are in grey.

## 4. Summary and conclusions

An study of the charge sharing in AC-LGADs from several angles of approach has been shown. The impact of $n^+$ layer resistivity and metal electrode pitch on the charge sharing and achievable position resolution is evident, favoring higher resistivities and to some extent narrower pitches. In all studied sensors, charge sharing enabled the determination of a significantly better position resolution than would be the case for a conventional DC-LGAD sensor. The charge sharing between neighboring strips has been examined in more detail, hinting at the induction of signal charge on several strips and subsequent re-sharing over the $n^+$ layer and prompting further thorough investigation in the future. Furthermore, an investigation of signal sharing over large distances through pulse height and timing cuts has been initiated.

Parameters such as $n^+$ layer implant concentration or resistivity, dielectric material and thickness vary between manufacturers, and this information is often proprietary. Often, the strip metal width and strip pitches are not identical either. Therefore it is challenging to directly (quantitatively) compare AC-LGAD sensors from different vendors, and the comparison of results remains on the level of individual cases.

While charge sharing between electrodes is one of the fundamental properties of AC-LGADs and an important motivation for their use in future 4D tracking detectors, distribution of the signal charge over a wider area than the very next neighbors is not desirable, as this would "blind" large areas of the sensor by a single hit and degrade timing and position resolution. It is observed that for strips with narrow pitch (and consequently, smaller gap in the metal), the second neighbor still contributes to a significant fraction of the signal (ca. 5%). Thus, a pitch of 100 $\mu$m is likely too small for most applications, and instead a pitch of at least 150-200 $\mu$m would be more suitable. Sparser segmentation of the sensor would also be favorable in terms of a reduced number of readout channels, translating into more relaxed spatial constraints and lower power consumption of the readout electronics. Sensors from a newer production, featuring even wider pitches of 300 and 500 $\mu$m, are currently under investigation.

## Acknowledgements

We thank the Fermilab accelerator and FTBF personnel for the excellent performance of the accelerator and support of the test beam facility, in particular M. Kiburg, E. Niner and E. Schmidt. We also thank the SiDet department for preparing the readout boards by mounting and wirebonding the AC-LGAD sensors. Finally, we thank L. Uplegger for developing the telescope tracker and a large part of the DAQ system. This study was conducted using the resources of the Fermi National Accelerator Laboratory (Fermilab), a U.S. Department of Energy, Office of Science, HEP User Facility. Fermilab is managed by the Fermi Research Alliance, LLC (FRA), acting under Contract No. DE-AC02-07CH11359. This research is partially funded by the U.S.-Japan Science and Technology Cooperation Program in High Energy Physics, through Department of Energy under FWP 20-32 in the USA, and via High Energy Accelerator Research Organization (KEK) in Japan. This work was also supported by the U.S. Department of Energy under grant DE-SC0010107-005; used resources of the Center for Functional Nanomaterials, which is a U.S. DOE Office of Science Facility, at Brookhaven National Laboratory under Contract No. DE-SC0012704; supported by the Chilean ANID PIA/APOYO AFB180002 and ANID - Millennium Science Initiative Program - ICN2019-044. This research was partially supported by Grant-in-Aid for scientific research on advanced basic research (Grant No. 19H05193, 19H04393, 21H0073 and 21H01099) from the Ministry of Education, Culture, Sports, Science and Technology, of Japan. J. Ott would like to acknowledge funding from the Finnish Cultural Foundation through the Postdoc Pool of Finnish Foundations.

## References

[1] H. F.-W. Sadrozinski, A. Seiden, N. Cartiglia,

, Reports on Progress in Physics 81 (2) (2017) 026101. doi:10.1088/1361-6633/aa94d3.
URL

[2] CMS Collaboration, A MIP Timing Detector for the CMS Phase-2 Upgrade, Tech. Rep. CERN-LHCC-2019-003. CMS-TDR-020, CERN, Geneva (Mar 2019).
URL `https://cds.cern.ch/record/2667167`

[3] ATLAS Collaboration, Technical Design Report: A High-Granularity Timing Detector for the ATLAS Phase-II Upgrade, Tech. Rep. CERN-LHCC-2020-007. ATLAS-TDR-031, CERN, Geneva (Jun 2020).
URL `https://cds.cern.ch/record/2719855`

[4] M. Tornago, R. Arcidiacono, N. Cartiglia, M. Costa, M. Ferrero, M. Mandurrino, F. Siviero, V. Sola, A. Staiano, A. Apresyan, K. Di Petrillo, R. Heller, S. Los, G. Borghi, M. Boscardin, G.-F. Dalla Betta, F. Ficorella, L. Pancheri, G. Paternoster, H. Sadrozinski, A. Seiden, Resistive ac-coupled silicon detectors: Principles of operation and first results from a combined analysis of beam test and laser data, Nucl. Instrum. Methods. Phys. Res. A 1003. doi:https://doi.org/10.1016/j.nima.2021.165319.
URL `https://www.sciencedirect.com/science/article/pii/S016890022100303X`

[5] G. Giacomini, W. Chen, G. D'Amen, A. Tricoli, Fabrication and performance of AC-coupled LGADs, Journal of Instrumentation 14 (09) (2019) P09004–P09004. doi:10.1088/1748-0221/14/09/p09004.
URL `http://dx.doi.org/10.1088/1748-0221/14/09/P09004`

[6] R. Heller, C. Madrid *et al.*, Characterization of BNL and HPK AC-LGAD sensors with a 120 GeV proton beam (2022). arXiv:2201.07772.
URL `https://arxiv.org/abs/2201.07772`

[7] K. Nakamura, S. Kita, T. Ueda, K. Hara, H. Suzuki, First Prototype of Finely Segmented HPK AC-LGAD Detectors, Proceedings of the 29th International Workshop on Vertex Detectors (VERTEX2020)arXiv:https://journals.jps.jp/doi/pdf/10.7566/JPSCP.34.010016, doi:10.7566/JPSCP.34.010016.
URL `https://journals.jps.jp/doi/abs/10.7566/JPSCP.34.010016`

[8] Fermilab Test Beam Facility.
URL `https://ftbf.fnal.gov`

[9] S. M. Mazza et al, Development of AC-LGADs for large-scale high-precision time and position measurements, IEEE Transactions on Nuclear Science (2022) submitted.